Viscoelastic Properties of Entangled Star Polymer Melts: Comparison of Theory and Experiment

Daniel A. Vega,[†,§] John M. Sebastian,[†,||] William B. Russel,[‡] and Richard A. Register[*,‡]

Department of Chemical Engineering and Princeton Materials Institute, Princeton University, Princeton, New Jersey 08544

Received August 20, 2001

ABSTRACT: We determine the linear viscoelastic properties of star polymer melts through an exact solution to the first-passage time expression developed by Milner and McLeish [*Macromolecules* **1997**, *30*, 2159] (MM), and compare with both the approximate solution proposed by MM and experimental data. The approximate and exact solutions show quite similar scalings of the terminal relaxation time with the number of entanglements per star arm n_e, with only a modest shift in time scale, accounting for the success of the approximate solution in treating moderately entangled stars. We also calculate the n_e dependence of the recoverable shear compliance and the zero-shear viscosity and compare these with extensive data taken from the literature. Zero-shear viscosities for stars of four different monomer chemistries and a range of n_e values are accurately represented by the MM theory, using plateau moduli and monomeric friction coefficients in good agreement with literature values.

Introduction

The viscoelastic behavior of entangled linear polymers is well described qualitatively by the reptation model originally proposed by de Gennes[1] and extended by Doi and Edwards.[2−4] In linear polymer melts of high molecular weight, the entanglement network may be modeled as a confining tube, which restricts chain diffusion to occur along the tube contour. However, the addition of long branches to a polymer (in architectures such as stars, combs, H-shaped polymers, or simply dangling chains in a polymer network) radically alters its dynamic behavior.[6−12] The branch points prevent reptation, and effects such as arm retraction,[4−6] contour length fluctuations[4] and dynamic dilution[13,14] that were neglected in the original treatment for linear polymers are key to a proper description of the dynamics of branched polymer melts. These concepts and their limitations are summarized in recent reviews.[14,15]

The simplest branched polymer architecture is a monodisperse star-shaped molecule composed of $f > 2$ equal arms, radiating from a central branch point. Such polymers have the unusual property that the viscosity increases exponentially with the molecular weight of the arms,[1,4−6,13−14] rather than following a power law as for linear polymers. Star polymers renew their configurations chiefly through arm retraction,[4] a process in which the end of each arm independently retracts partway down its confining tube and then reemerges along a different trajectory. The time required for a chain to first retract a certain distance along its tube contour is termed the "first-passage time" (FPT).[6,14] Recently, Milner and McLeish (MM) have presented a complete theory for the stress relaxation of star polymer melts, whose only material-dependent parameters are obtainable from independent measurements on linear polymers.[14] In addition, some aspects of this theory have been applied successfully to polymers of other architectures ("pompom" polymers,[9] H-polymers,[10] and star-linear polymer blends[16]). The theory couples the basic arm retraction mechanism with constraint relaxation (dynamic dilution of the entanglement network), and provides a good quantitative description of dynamic rheological data for melts of polybutadiene ($f = 4$, 12)[8,14] and polyisoprene ($f = 4$)[8,14,17] stars. However, to obtain the best fits to experimental data, the calculated dynamic moduli $G^*(\omega)$ must be shifted by a modest but apparently systematic factor ($\approx$2) to lower frequencies.[8,14,17]

To obtain a closed-form expression for the FPT, Milner and McLeish[14] developed approximate solutions to the integrals defining the FPT; these approximations are valid in the limit of high arm molecular weight. However, because of the exponential dependence of relaxation time on arm length, this limit is experimentally difficult to reach, and much of the extant data corresponds to stars whose arms are only lightly or moderately entangled (number of entanglements per arm, n_e, <20 and often <5).[8,17] We first present an exact solution to the FPT problem as formulated by Milner and McLeish, which allows for an assessment of the validity of the approximations made in the original solution. We then proceed to calculate other experimentally accessible viscoelastic functions (frequency and magnitude of the maximum in loss modulus, $G''(\omega_{max})$; recoverable compliance, J_e^0; zero-shear viscosity, η_0) from the exact solution to the MM model and compare their dependence on n_e with literature data for well-characterized stars.

Milner-McLeish (MM) Theory for Star Polymer Melts. Employing the concept of dynamic dilution, MM showed that the relaxation modulus $G(t)$ for star polymer melts can be expressed as[14]

$$G(t) = G_0(1 + \alpha)\int_0^1 \mathrm{d}s(1 - s)^{\alpha} \exp[-t/\tau(s, n_e)] \quad (1)$$

* Corresponding author. E-mail: register@princeton.edu.
† Department of Chemical Engineering, Princeton University.
‡ Princeton Materials Institute, Princeton University.
§ Permanent address: Department of Physics, Universidad Nacional del Sur, Av. Alem 1253, 8000-Bahia Blanca, Argentina.
|| Present address: 3M Corporate Research, Science Research Center, St. Paul, MN 55144-1000.

10.1021/ma011501n CCC: $22.00
Published on Web 11/27/2001

where s is the fractional distance which the free end of the arm has retracted down the tube ($s = 0$ for the initial, unrelaxed state at time $t = 0$; $s = 1$ for the fully retracted, fully relaxed state), $\tau(s, n_e)$ is the characteristic time for the arm to retract a distance s, and $\alpha = {}^4/_3$ is the Colby−Rubinstein dilution exponent.[18] The number of entanglements per star arm n_e is related to the molecular weight between entanglements M_e and the arm molecular weight M_a as $n_e = M_a/M_e$. The complex dynamic modulus $G^*(\omega)$ can be expressed as[14]

$$G^*(\omega) = G_0(1 + \alpha)\int_0^1 ds(1 - s)^\alpha\left[\frac{-i\omega\tau(s, n_e)}{1 - i\omega\tau(s, n_e)}\right] \quad (2)$$

The retraction of the chains, and thus the relaxation spectrum $\tau(s, n_e)$, divides into two distinct regimes. First, at early times (or high frequencies) the motion of the arm's free end is governed by the longitudinal Rouse modes of a semi-infinite chain. The time for this fast process $\tau_f(s, n_e)$ can be expressed as[14,17,19]

$$\tau_f(s, n_e) = (225\,\pi^3/256)\tau_e n_e{}^4 s^4 \quad (3)$$

where τ_e is the Rouse time of an entanglement segment (having molecular weight M_e). Second, at longer times (or lower frequencies), the slow arm retraction process is characterized by the time $\tau_s(s, n_e)$, which MM determined[14] by solving the FPT problem as

$$\tau_s(s, n_e) = \left(\frac{L^2}{D_{eff}}\right)\int_0^s ds' \exp[U(s', n_e)]\int_{-\infty}^{s'} ds'' \exp[-U(s'', n_e)] \quad (4)$$

where s' and s'' are integration variables and

$$U(s, n_e) = \frac{15}{4}n_e\frac{1}{(1 + \alpha)(2 + \alpha)}[1 - (1 - s)^{1+\alpha}(1 + (1 + \alpha)s)] \quad (5)$$

is the effective potential for arm retraction, D_{eff} is the effective diffusion coefficient, and L is the tube length.

To evaluate τ_s from eq 4, MM noted that the inner integral is dominated by the region near $s'' = 0$ and approximated it with a constant

$$\int_{-\infty}^{s'} ds \exp[-U(s, n_e)] \approx \sqrt{\pi/(2U''(0, n_e))} \quad (6)$$

where $U''(0, n_e) = d^2U(s, n_e)/ds^2|_{s=0}$. As for the outer integral, MM considered the form of the potential U both near and far from $s = 1$ and wrote approximate expressions for each, which are combined through a simple crossover function to yield the following expression[17] for all s

$$\tau_s(s, n_e) \approx \tau_e n_e{}^{3/2}\left[\frac{\pi^5}{30}\right]^{1/2} \frac{\exp[U(s, n_e)]}{s\left\{(1 - s)^{2\alpha} + \left[\frac{4}{15\,n_e}(1 + \alpha)\right]^{2\alpha/1+\alpha}\Gamma[1/(1 + \alpha)]^{-2}\right\}^{1/2}} \quad (7)$$

Finally, MM unite the early-time (eq 3) and the late-time (eq 7) expressions through another crossover formula[14,17]

$$\tau_s(s, n_e) = \frac{\tau_f(s, n_e)\exp[U(s, n_e)]}{1 + \tau_f(s, n_e)\exp[U(s, n_e)]/\tau_s(s, n_e)} \quad (8)$$

If $n_e \gg 1$, this expression reduces to eq 3 at short times (small s) and to eq 7 at long times (large s), with the crossover occurring[14,17] at $s \approx \sqrt{1/n_e}$.

The key result of the MM theory is the integral expression for the FPT, eq 4 (coupled with the Rouse result of eq 3 through the crossover formula, eq 8). The approximations made in going from eq 4 to eq 7 (which we will term the "approximate solution" below) are convenient but not necessary. In the following section we present the exact solution (an infinite series) to the FPT as formulated by MM (eq 4), and compare it with the approximate solution (eq 7).

Results and Discussion

Exact Solution to the FPT. For notational simplicity, we define

$$q_1 = \frac{15}{4}n_e\frac{1}{1 + \alpha} \quad (9a)$$

$$q_2 = \frac{15}{4}n_e\frac{1}{2 + \alpha} \quad (9b)$$

The exponential term in the inner integral of eq 4 may then be expressed as a power series in $(1 - s)$ as

$$\exp[-U(s, n_e)] = \exp[-U(1, n_e)]\sum_{k=0}^{\infty}[q_2(1 - s) + q_1]^k\frac{(1 - s)^{k(1+\alpha)}}{\Gamma(k + 1)} \quad (10)$$

Integrating the potential given by eq 10 yields, for the inner integral $I_1(s, n_e)$

$$I_1(s, n_e) = \int ds' \exp[-U(s', n_e)] = \exp[-U(1, n_e)]\sum_{k=0}^{\infty}A_k(1 - s)^{k(1+\alpha)+1}\,{}_2F_1(-k, \hat{k} + 1; \hat{k} + 2; -\hat{s}) \quad (11)$$

where ${}_2F_1(\alpha_1, \alpha_2, ..., \alpha_p; \beta_1, \beta_2, ..., \beta_q; z)$ is the generalized hypergeometric series,[20] $\hat{s} = q_2(1 - s)/q_1$, $\hat{k} = k(1 + \alpha)$, and

$$A_k = \frac{{q_1}^k}{(\hat{k} + 1)\Gamma(k + 1)} \quad (12)$$

Similarly, the exponential in the outer integral of eq 4 may be expressed as

$$\exp[U(s, n_e)] = \exp[U(1, n_e)]\sum_{k=0}^{\infty}(-1)^k[q_2(1 - s) + q_1]^k\frac{(1 - s)^{\hat{k}}}{\Gamma(k + 1)} \quad (13)$$

Taking the product of eq 11 evaluated between $-\infty$ and

s' and the series given by eq 13, the characteristic time $\tau_s(s, n_e)$ may be expressed as

$$\tau_s(s, n_e) = L_1 \sum_{k=0}^{\infty} (-1)^k [q_2(1 - s) + q_1]^k \frac{(1 - s)^{\hat{k}}}{\Gamma(k + 1)} - \Lambda(s, n_e) \quad (14)$$

where

$$L_1 = \lim_{s \to -\infty} \sum_{k=0}^{\infty} A_k (1 - s)^{\hat{k}+1} \, {}_2F_1(-k, \hat{k} + 1; \hat{k} + 2; -\hat{s}) \quad (15)$$

and

$$\Lambda(s, n_e) = \int_0^s ds' \, \Xi(s', n_e) \quad (16)$$

with

$$\Xi(s, n_e) = \sum_{k=0}^{\infty} \sum_{n=0}^{k} \sum_{h=0}^{k-n} B_{k,n,h} \, \hat{s}^{\hat{k}+h+1} \, {}_2F_1(-n, \hat{n} + 1; \hat{n} + 2, -\hat{s}) \quad (17)$$

where $\hat{n} = n(1 + \alpha)$. The coefficients $B_{k,n,h}$ in $\Xi(s, n_e)$ can be expressed as

$$B_{k,n,h} = (-1)^{k-n} \frac{q_1^{k+1}}{q_2} \binom{k - n}{h} \frac{1}{[\hat{n} + 1]n![k - n]!} \quad (18)$$

Finally, the integral $\Lambda(s, n_e)$ in eq 16 can be written as

$$\Lambda(s, n_e) = - \sum_{k=0}^{\infty} \sum_{n=0}^{k} \sum_{h=0}^{n-k} C_{k,n,h} \, \hat{s}^{k+h+2} \, \Theta_{k,n,h}(\hat{s}) \quad (19)$$

where $\Theta_{k,n,h}(\hat{s})$ is related to the generalized hypergeometric series as

$$\Theta_{k,n,h}(\hat{s}) = {}_3F_2(\hat{k} + h + 2, -n, \hat{n} + 1; \hat{k} + h + 3, \hat{n} + 2; -s) \quad (20)$$

and the coefficients $C_{k,n,h}$ are given by

$$C_{k,n,h} = - \frac{q_1}{q_2} \frac{1}{\hat{k} + h + 2} \quad (21)$$

In Figure 1, we compare the numerical integration of the inner integral in eq 4 and the analytical result given by eq 11, taking 10 and 20 terms of the series for $n_e = 4$ and $n_e = 10$, respectively. The agreement is excellent. Figure 1 also shows that the approximation employed in eq 6 ($I_1(s, n_e) =$ constant for $s > 0$) is valid only for $n_e \gg 1$, whereas the values of $n_e = 4$ and 10 shown are typical for star polymers studied experimentally.

Figure 2 shows $\tau_s(s, n_e)/\tau_s(1, n_e)$ as given by the approximate form in eq 7 for different values of n_e, focusing on the long-time region ($s \approx 1$). The calculated curves show a maximum in $\tau_s(s, n_e)$ for $s < 1$, which is clearly nonphysical: it implies that a longer time is required for the chain to retract partway down the tube than all the way down the tube. The maximum becomes progressively less pronounced as n_e is increased, but is still clearly evident at $n_e = 15$. This maximum is a consequence of the approximations made in reaching eq 7 and is not present in the exact solution. Figure 3 shows the behavior of $\tau(s, n_e)/\tau(1, n_e)$ as given by the crossover formula in eq 8, for $n_e = 5$ and $n_e = 10$ over the entire range of s. The open symbols correspond to the approximate solution and show the same maximum as in Figure 2, while the exact results (20 terms of the series) for the same cases are presented as the filled symbols and increase monotonically toward $s = 1$. For comparison, $\tau(s, n_e)$ was also evaluated by numerical integration of eq 4 (continuous curves). The analytical and numerical results are indistinguishable, again confirming that 20 terms of the series were sufficient.

However, normalization by the terminal relaxation time $\tau_0 = \tau(s, n_e)$ obscures an important result. The inset to Figure 3 presents the approximate and exact solutions for $n_e = 8$ without normalizing by τ_0. At low s, the approximate and exact solutions must be identical because the same expression for the early-time process (τ_f from eq 3) and the same crossover formula (eq 8) were

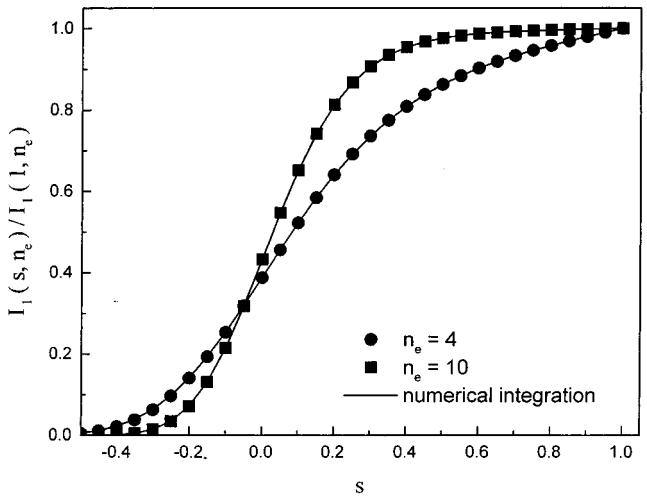

Figure 1. Exact solution to the inner integral in the first-passage time (FPT) problem, $I_1(s,n_e)$, normalized by the value at $s = 1$ (complete retraction), for $n_e = 4$ (circles, 10 terms in series) and $n_e = 10$ (squares, 20 terms in series). Numerical evaluations of the same integrals are shown as the continuous curves.

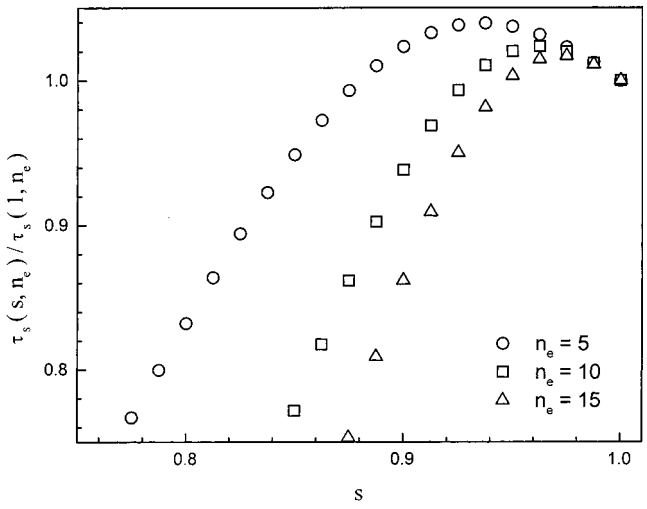

Figure 2. Normalized FPT $\tau_s(s, n_e)/\tau_s(1, n_e)$, as given by the approximate solution to the MM theory (eq 7) for different values of n_e.

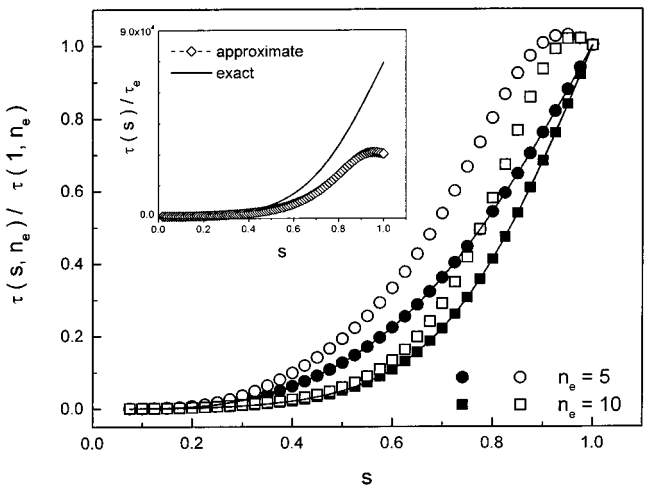

Figure 3. Relaxation time $\tau(s, n_e)$ as defined by eq 8, normalized by the terminal time $\tau(1, n_e)$, as given by the approximate solution (open symbols), exact solution (filled symbols), and numerical integration of eq 4 (continuous curves). Results are presented for $n_e = 5$ and 10. Inset: $\tau(s)$ for $n_e = 8$, without normalizing by the terminal time, giving the approximate solution (open diamonds) and exact solution (continuous curve). In the inset, $\tau(s)$ is normalized by the basic microscopic time τ_e (Rouse time of an entanglement segment), common to both approximate and exact solutions.

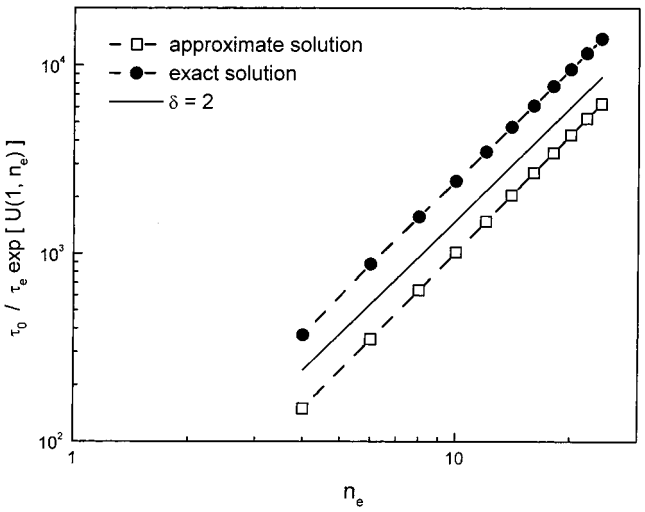

Figure 4. Preexponential dependence of the terminal relaxation time τ_0 on the number of entanglements per star arm, n_e. The exponential dependence of τ_0 on n_e has been normalized out to more clearly reveal the form of the preexponential factor. Key: open squares, approximate solution; filled circles, exact solution. Solid line, shown for comparison, corresponds to a power-law exponent $\delta = 2$.

used for both. By contrast, for s $\approx$ 1, the exact and approximate solutions for $\tau(s, n_e)$ differ by roughly a factor of 2, meaning that the approximate expression underpredicts the terminal time by a factor of 2 when $n_e = 8$.

Scaling of Terminal Relaxation Time with Arm Molecular Weight. An important quantity to extract from any theory of star polymer behavior is the dependence of the terminal relaxation time τ_0 on n_e. The early Doi−Kuzuu (DK) theory, which modeled arm retraction in a fixed network, predicted that τ_0 should increase exponentially with the number of entanglements per star arm and have a power-law preexponential factor[4,5]

$$\tau_0 \sim n_e^{\delta} \exp[\phi n_e] \tag{22}$$

where Doi and Kuzuu predicted $\delta = 3$ and $\phi = {}^{15}/_{8}$, while the subsequent lattice model treatment of Pearson and Helfand (PH)[6,21] yielded $\delta = {}^{3}/_{2}$ and $\phi = 0.6$. The exact value of ϕ predicted by the PH model depends on the lattice coordination number; the value of 0.6, which was chosen to agree with experimental data, corresponds to a lattice coordination number[11] of approximately 12. Though ϕ was determined empirically, the PH model provides a good quantitative description of the n_e dependence of the zero-shear viscosity η_0 of star melts,[6] so any parameter-free theory (such as that of MM) would be expected to produce results of a similar form.

The outer integral in eq 4 shows that the terminal relaxation time ($s = 1$) should have an exponential dependence on U; from eq 5 with $\alpha = {}^{4}/_{3}$, at $s = 1$, we obtain $U(1,n_e) = (27/56)n_e$, and so anticipate $\phi = 27/56 \approx 0.48$. To evaluate δ, Figure 4 shows the terminal time τ_0, normalized by $\tau_e \exp[U(s = 1, n_e)]$, as a function of n_e. Results are calculated from eq 8 using both the approximate (eq 7) and exact (eq 14) expressions. The results from both expressions are indeed well-represented by power laws, with best-fit exponents of 1.98 (exact solution) and 2.08 (approximate solution) over the range $5 \le n_e \le 24$. Thus the scaling of the terminal time with n_e is well represented by

$$\tau_0/\tau_e \exp[U(s = 1, n_e)] \sim n_e^{\,2} \tag{23}$$

Or in unnormalized form

$$\tau_0 \sim n_e^{\,2} \exp\left[\frac{27}{56} n_e\right] \tag{24}$$

Equation 24 has the same form as the DK and PH results, but with a slightly smaller exponential factor ϕ and larger power-law exponent δ than given by PH.

Simple extrapolation of the power-law fits to the data of Figure 4 suggests that the approximate and exact solutions for τ_0 will only approach convergence for n_e of order 10^4, far outside the experimentally accessible range. The close similarity in the scaling behavior exhibited by the approximate and exact solutions means that, over the practical range of n_e, the factor-of-two underestimate of τ_0 revealed in the inset to Figure 3 holds for all values of n_e. This provides an explanation for the frequency shifts (factor-of-2 to lower frequency) which have been found necessary to achieve the best match of the approximate solution to the MM model with experimental $G^*(\omega)$ data.[8,14,17]

Dynamic Moduli. Figure 5 shows the stress relaxation curve and dynamic moduli calculated using eqs 1 and 2, for both the approximate and exact solutions to the MM model, with parameter values $n_e = 6$, $G_0 = 0.6$ MPa, and $\tau_e = 15$ s (parameters corresponding to high-1,4 polyisoprene at its quasistatic glass transition temperature[8]). The exact and approximate solutions coincide at high frequencies (short times), as expected, but differ significantly in the terminal region. Echoing the results of the preceding section, the approximate solution predicts a terminal relaxation that occurs at approximately half the time (twice the frequency) of the exact solution. Consequently, the approximate solution yields a relaxation spectrum which is too narrow, as seen by the breadth of the maximum in $G''(\omega)$.

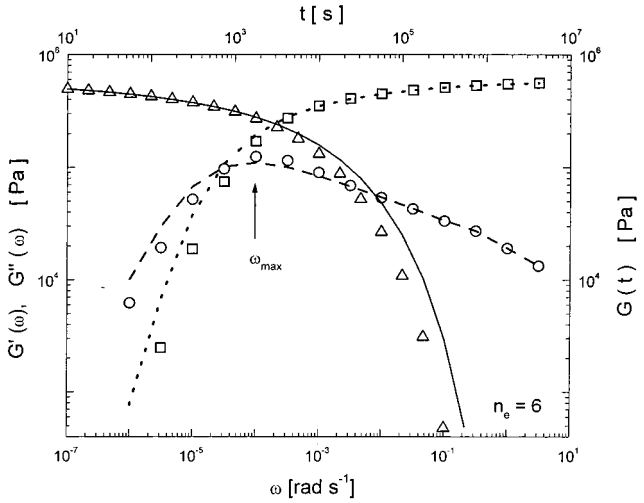

Figure 5. Linear viscoelastic moduli predicted by the approximate solution (symbols) and exact solution (lines) to the MM theory. Results calculated with representative parameters, $n_e = 6$, $G_0 = 0.6$ MPa, $\tau_e = 15$ s. Left axis: squares and dotted line, $G'(\omega)$; circles and dashed line, $G''(\omega)$. Right axis: triangles and solid line, $G(t)$.

Table 1. Scaling Exponents in $\tau_{max} \sim n_e^{\gamma}$ Based on Literature Data

star polymer	f	γ	range[a] of n_e	ref
polyisoprene	4	2.6	2.3−21	28
polybutadiene	4	2.1	7−64	22
polystyrene	4	2.8	1.7−23	23
polystyrene	6	2.9	6−13	23

[a] Calculated with values of M_e derived from plateau modulus and density data in ref 24.

While $G^*(\omega)$ contains all the information on the relaxation dynamics, it is frequently convenient to extract single parameters from $G^*(\omega)$, rather than working with the entire spectrum. Moreover, experimentally it may be possible to capture only a portion of the relaxation spectrum for a particular material. Two important parameters derived experimentally from measurements in the terminal region are the recoverable shear compliance J_e^0 and the zero-shear viscosity η_0. In the higher-frequency region, the maximum in $G''(\omega)$ has been a focus of experimental study, characterizing how both its location ω_{max} (indicated by the arrow in Figure 5) and magnitude $G''(\omega_{max})$ vary with arm molecular weight. In the following sections, we calculate these functions from the MM theory and compare the results with literature data for well-characterized stars.

Maximum in Loss Modulus. Roovers[22] has suggested that the time defined by $\tau_{max} = 1/\omega_{max}$ should scale with n_e^2, corresponding to a Rouse-like relaxation. Note that this n_e^2 dependence is embodied in eq 3, since the relevant values of s for the fast process extend only up to the crossover point, $s \approx \sqrt{1/n_e}$. Experimentally,[22,23] τ_{max} has been found to exhibit a slightly stronger power-law dependence on n_e

$$\tau_{max} \sim n_e^{\gamma} \tag{25}$$

where $2 < \gamma < 3$ (see Table 1), though the range of n_e available for each fit is only a decade or so. Figure 6 shows the calculated dependence of τ_{max} on n_e according to the MM model (both approximate and exact solutions). For well-entangled arms ($10 \le n_e \le 22$), the

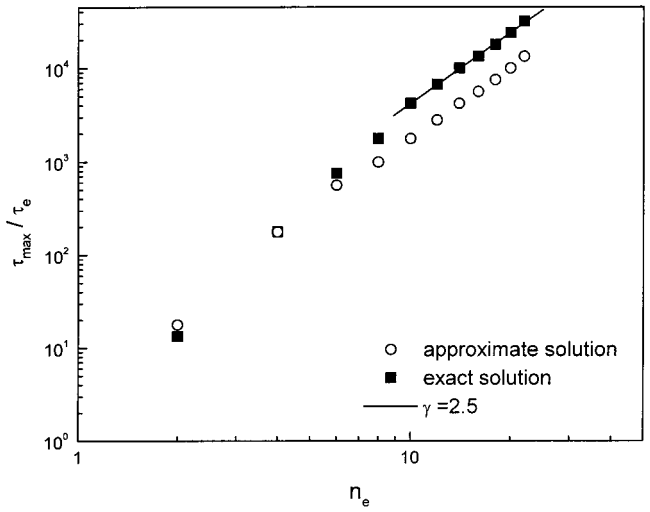

Figure 6. Reciprocal of the frequency at the peak of $G''(\omega)$, denoted as τ_{max}, vs n_e as predicted by the MM model (filled squares, exact solution; open circles, approximate solution). τ_{max} is normalized by the basic microscopic time τ_e (Rouse time of an entanglement segment). The solid line is a power-law fit to the data at high n_e, with an exponent $\gamma = 2.5$.

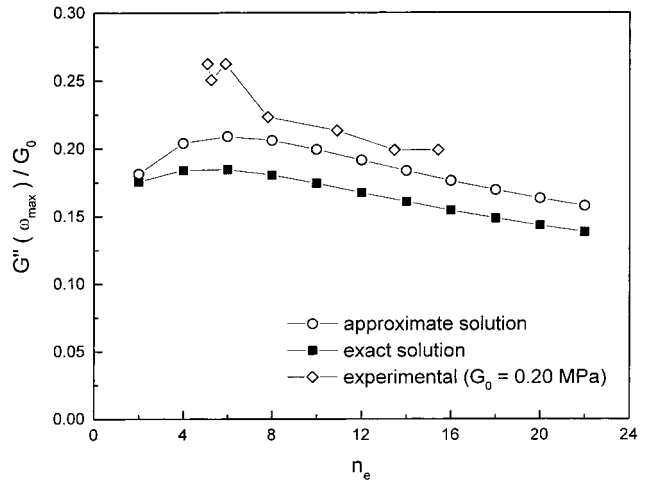

Figure 7. Magnitude of $G''(\omega_{max})$ as a function of n_e as predicted by the model (filled squares: exact solution; open circles: approximate solution). $G''(\omega_{max})$ is normalized by the plateau modulus G_0. Open diamonds: data of Graessley and Roovers[23] for 4- and 6-arm star polystyrenes, normalized by $G_0 = 0.20$ MPa.

results are well described by eq 25 with $\gamma = 2.5$, in good agreement with the experimental exponents given in Table 1. For less-entangled arms, a larger apparent power-law exponent is predicted (Figure 6).

Since the maximum in G'' is merely part of a continuous distribution of relaxations including both Rouse and arm retraction processes (see Figure 5), it is not surprising that ω_{max} does not precisely follow Rouse-like behavior. But the similarity in behavior ($\gamma = 2.5$ vs 2) is not coincidental: for well-entangled arms, the G'' maximum occurs toward the high-frequency end of the relaxation spectrum, where it is heavily influenced by the Rouse-like relaxations. Indeed, MM showed[14] the need to incorporate the spectrum of Rouse modes (rather than just the lowest mode) to obtain an accurate description of the shape of G'' in the region of the maximum.

From the MM theory, we can also calculate the magnitude of $G''(\omega_{max})$, which is shown in Figure 7. The peak height corresponds to roughly 1/6 of the plateau

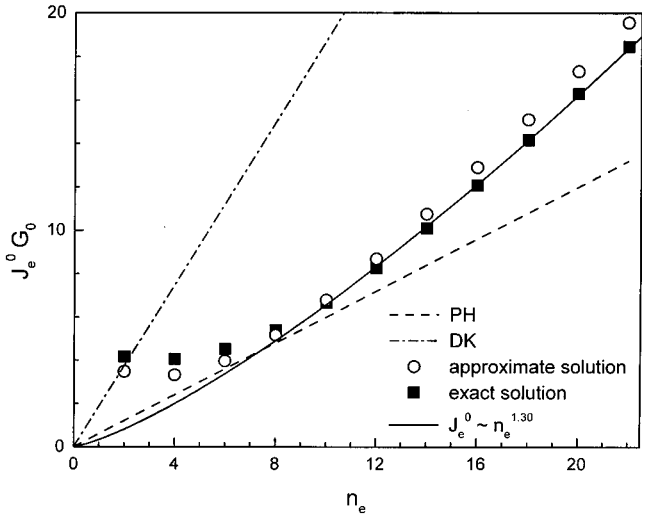

Figure 8. $J_e^0 G_0$ vs the number of entanglements per star arm n_e, calculated from both the approximate (open circles) and exact (filled squares) solutions to the MM theory. Lines shown for comparison represent $\phi = {}^{15}/_{8}$ (DK theory, dot−dashed line), 0.6 (PH theory, dashed line), and a power-law dependence with exponent $\kappa = 1.30$ (best-fit to the exact MM results for $10 \leq n_e \leq 24$, solid line).

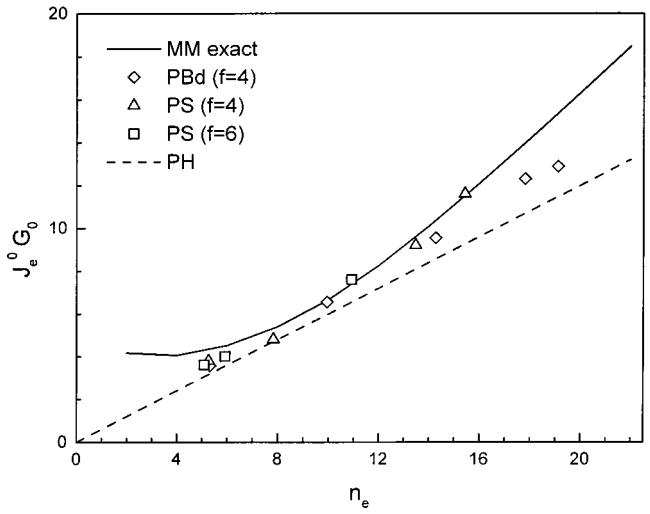

Figure 9. Experimental values of $J_e^0 G_0$ vs the number of entanglements per star arm n_e. Key: diamonds, four-arm polybutadiene stars;[22] triangles, four-arm polystyrene stars;[23] squares, six-arm polystyrene stars.[23] Predictions of the PH theory (dashed line) and MM theory (exact solution, solid line) are shown for comparison. G_0 values employed[24] were 1.15 MPa for polybutadiene and 0.20 MPa for polystyrene.

modulus G_0, though the theory predicts a systematic decrease with n_e for $n_e > 5$. Such a systematic decrease has been observed experimentally by Graessley and Roovers[23] in a series of 4- and 6-arm star polystyrenes. For comparison, these experimental data are plotted in Figure 7, normalized by $G_0 = 0.20$ MPa.[24] The slopes of the theoretical and experimental curves are quite similar for well-entangled stars ($n_e \geq 8$); good quantitative agreement could be obtained if $G_0 = 0.25$ MPa were used for normalization, but this lies somewhat outside the range of experimental data for polystyrene. This modest quantitative discrepancy may reflect a deficiency in the ad hoc crossover formula (eq 8) used in constructing $\tau(s,n_e)$ from the Rouse and FPT results, as τ_{max} falls in the vicinity of the crossover point.

Recoverable Shear Compliance. Another important rheological parameter, the recoverable shear compliance J_e^0, is related to the relaxation modulus through[25]

$$J_e^0 = \frac{\int_0^\infty G(t)\, t\, dt}{[\int_0^\infty G(t)\, dt]^2} \tag{26}$$

Experimentally,[4,6,15] J_e^0 for star polymer melts increases roughly linearly with molecular weight, even for $n_e \gg 1$, rather than reaching a plateau as for monodisperse linear polymers. This agrees with theories for the relaxation of star polymers in a network of fixed entanglements, which predict

$$J_e^0 G_0 \approx \phi n_e \tag{27}$$

with $\phi = {}^{15}/_{8}$ in the DK theory[5] and $\phi = 0.6$ in the PH theory.[6] Figure 8 shows the predictions of the MM theory (both approximate and exact solutions) for $J_e^0 G_0$. For $n_e > 4$, the MM theory shows this same general trend of a steady increase in $J_e^0 G_0$ with n_e; the approximate solution predicts a slightly more rapid increase. For $n_e \geq 10$, the results from the exact solution to the MM theory are well-represented by a power law

$$J_e^0 G_0 \sim n_e^{\kappa} \tag{28}$$

with $\kappa = 1.30$, a slightly stronger dependence than predicted by the DK and PH theories.

The deviations observed from this power-law behavior for small values of n_e (in particular $n_e \leq 6$) appear to result initially from a failure of the crossover formula, eq 8. Indeed, eq 8 requires the behavior to cross over to that predicted by arm retraction (eq 4 for the FPT), even for arms so short that the dynamics should be essentially Rouse-like for all s. While one could propose alternative formulas to replace eq 8 and extend to somewhat lower n_e the range over which J_e^0 is accurately predicted, a more fundamental problem is encountered at small n_e: the breakdown of the dynamic dilution idea, which rests upon a separation of time scales between that for relaxation of entanglement constraints by the motion of confining chains and for relaxation via arm retraction.[14]

The small difference in power law exponent between eqs 27 and 28 (1.30 vs 1) would be difficult to discern experimentally, especially as literature data for J_e^0 on star polymer melts are limited. Figure 9 shows the data of Roovers[22] for polybutadiene melts ($f = 4$) and of Graessley and Roovers[23] for polystyrene melts ($f = 4$, 6), normalized with the G_0 values for linear polymers tabulated by Fetters et al.[24] Over the experimental range of $5 < n_e < 20$, the MM theory yields at least as good a representation of J_e^0 as does the PH theory; a quantitative comparison shows a 20% smaller sum of squared residuals between model and data when the MM model is used.

Note, however, that all these theories (DK, PH, and MM) predict that J_e^0 is independent of the number of arms in the star, f. Roovers[26] examined polybutadiene stars having 4, 18, and 32 arms; fits to eq 27 revealed a steady increase in ϕ with f, rising from 0.6 ($f = 4$) to 1.0 ($f = 18$) to 1.4 ($f = 32$). The data of Graessley and Roovers[23] for polystyrene melts with $f = 4$ and $f = 6$ are also well-represented[6] by $\phi = 0.6$. The results from

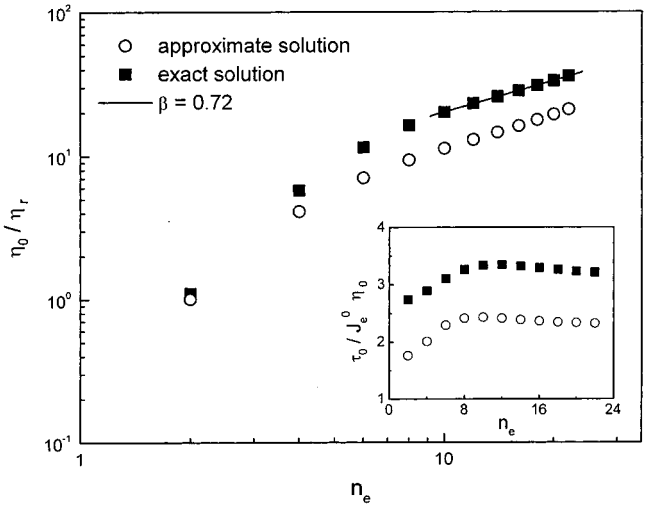

Figure 10. Scaling dependence of the zero-shear viscosity η_0 on the number of entanglements per star arm n_e, calculated from both the approximate (open circles) and exact (filled squares) solutions to the MM theory. Here, η_0 is normalized by the microscopic viscosity η_r defined in the text. Solid line shows a power-law dependence with $\beta = 0.72$. Inset: $\tau_0/J_e^0\eta_0$ calculated from both the approximate (open circles) and exact (filled squares) solutions to the MM theory.

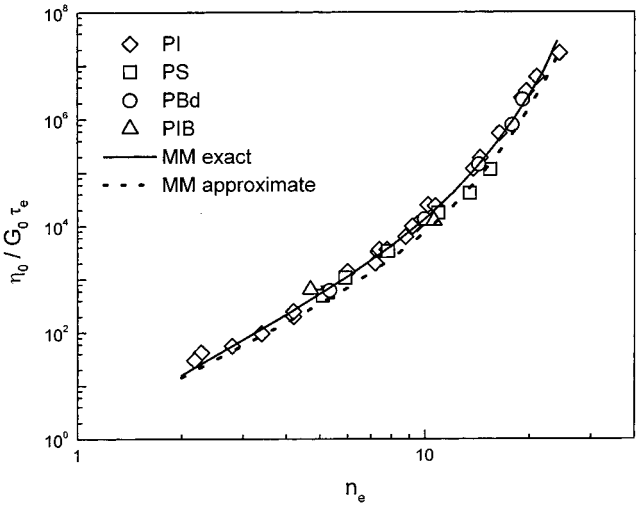

Figure 11. Comparison of experimental and theoretical values of the zero-shear viscosities of star polymers, presented in normalized form as $\eta_0/G_0\tau_e$ vs n_e. Key: solid line, MM theory, exact solution; dashed line, MM theory, approximate solution; diamonds, PI stars;[28] squares, PS stars;[23] circles, PBd stars;[22] triangles, PIB stars.[29] Parameters used in calculating G_0, τ_e, and n_e for the experimental data are given in Table 2.

the MM theory are broadly consistent with the values of ϕ found for $f = 4$ and even for $f = 18$, but not for $f = 32$. For very high functionality stars ($f \geq 64$), liquidlike ordering of the star molecules introduces an additional low-frequency relaxation process,[8,27] whose presence should raise J_e^0 and thus the apparent value of ϕ as defined by eq 27. It is plausible that this effect could be significant enough at $f = 32$ to produce a 50% increase in J_e^0; this subject merits further experimental investigation.

Zero-Shear Viscosity. The most keenly studied rheological parameter for star polymer melts is the zero-shear viscosity η_0, whose exponential increase with arm length has long been considered a distinctive feature of the star architecture.[4−6] The value of η_0 can be calculated from the relaxation modulus through[25]

$$\eta_0 = \int_0^\infty G(t)\,\mathrm{d}t \tag{29}$$

Figure 10 shows η_0, normalized by $\eta_r = G_0\tau_e/(1 + \alpha)$ exp$[U(s = 1, n_e)]$, as a function of n_e for both the approximate and exact MM solutions. The approximate solution yields values roughly a factor of 2 too low, consistent with the factor-of-two underestimation of τ_0 evident in Figure 4. For $n_e < 4$, the MM theory predicts a very rapid falloff of η_0, which has the same origin as the large values of J_e^0 predicted in this range of n_e (Figure 8).

Models for polymer dynamics often yield relationships between τ_0, J_e^0, and η_0 of the form

$$\tau_0 = a J_e^{\,0}\eta_0 \tag{30}$$

For monodisperse linear polymers, $a = 1$ for the unentangled case, and the tube model predicts $a = 10/\pi^2$ ($\approx$ 1.013) for the entangled case.[4,25] For stars, the DK[5] and PH[6] theories predict $a = 2$. If the MM theory were to also follow eq 30, then at high n_e, consistency with eqs 22 and 28 would require

$$\eta_0 \sim n_e^{\,\beta} \exp[\phi n_e] \tag{31}$$

where $\beta = \delta - \kappa \approx 1.98-1.30 = 0.68$ and $\phi = 27/56 \approx$ 0.48. The same form is predicted by the DK theory[5] ($\beta = 2$, $\phi = {}^{15}/_{8}$) and the PH theory[6] ($\beta = {}^{1}/_{2}$, $\phi = 0.6$). The best-fit power-law exponent to the results in Figure 10 (MM exact solution) for $n_e \geq 10$ is $\beta = 0.72$, close to the expected value of 0.68. However, the small difference in exponent is not a fitting artifact, and the inset to Figure 10 reveals its origin: the MM model predicts that $J_e^0\eta_0$ decreases weakly at high n_e. (Of course, since J_e^0 and η_0 are each determined by integrals over the relaxation distribution (eqs 26 and 29) there is no reason a as defined by eq 30 cannot be a function of n_e.) For the larger values of n_e in Figure 10, $\tau_0/J_e^0\eta_0 \approx 3.2$, greater than predicted by the DK and PH theories.

The keen focus on η_0 over the years provides a large body of experimental data against which to compare the predictions of the MM theory. The normalized viscosity $\eta_0/G_0\tau_e$ should be a universal function of n_e (see eq 29). This function, calculated from the exact solution for the MM theory, is shown as the solid curve in Figure 11; the dashed curve shows the prediction of the approximate solution, lying roughly a factor of 2 below the exact solution. To compare experimental data with this prediction, several other experimental quantities are required: the plateau modulus G_0; the entanglement molecular weight M_e, to calculate n_e from experimentally determined arm molecular weights; and the Rouse time per entanglement τ_e. The last of these may be calculated from[4,14]

$$\tau_e = \frac{1}{3\pi^2}\frac{\zeta N_e^{\,2} b^2}{k_B T} \tag{32}$$

where k_B is Boltzmann's constant and T is the absolute temperature. This expression contains three other material parameters which must be determined from experiment: the number of monomers per entanglement N_e ($=M_e/m_0$, where m_0 is the monomer molecular weight); the statistical segment length b, where b^2 is the mean-square end-to-end distance per monomer unit;

Table 2. Parameters Used in Comparing η_0 Data for Star Melts with Theory

star polymer[a]	T (K)	ρ (10^3 kg/m^3)	m_0 (g/mol)	b (nm)[24]	G_0, lit.[24] (MPa)	M_e, fitted (g/mol)[b,c]	G_0, fitted (MPa)[b,c]	log ζ, lit.[d] (10^3 (N s)/m)	log ζ, fitted (10^3 (N s)/m)[c]
PBd[22]	300	0.89	54.09	0.688	1.15	2120 ± 90	1.05 ± 0.04	−7.07[22]	−6.95 ± 0.09
PS[23]	442.5	0.95	104.15	0.672	0.20	16600 ± 800	0.21± 0.01	−4.95[30]	−4.83 ± 0.11
PI[28]	333	0.88	68.12	0.642	0.37	5000 ± 100	0.44 ± 0.01	−6.68[30]	−6.86 ± 0.08
PIB[29]	298	0.92	56.11	0.566	0.32	7700	0.29	−4.35[25]	−4.13

[a] The η_0 vs M_a data for each polymer type was taken from the reference indicated. [b] Fitted values of M_e and G_0 are not independent, but are related by Eq 33. [c] Quoted uncertainties are ±1 standard deviation of the best fit. [d] Adjusted from the published value to be consistent with the value of b quoted in this table; for PS and PI, also corrected to the values for high-molecular-weight polymer as described in the Appendix.

and the monomeric friction coefficient ζ. Additionally, G_0 and M_e are related through[4,25]

$$G_0 = \rho RT/M_e \tag{33}$$

where ρ is the mass density.

Values of ρ, b, G_0 (or M_e), and ζ are all given in the literature for a range of common polymers but not necessarily at the precision required for a discriminating comparison with the calculated curves in Figure 11. Of these four quantities, the precisions of the latter two are typically limiting: M_e, because of the very strong dependence of η_0 on n_e given by eq 31, and ζ, which is commonly considered to be known only within a factor of 2 or so.[14,22,25] However, if η_0 data exist for star polymers made from a single monomer over a sufficiently wide range of arm molecular weights, then M_e and ζ can be determined directly from the data by allowing the two to vary in order to produce the best match of the data to the theoretical curve shown in Figure 11. This is the approach we take here; subsequently, we compare the fitted values of M_e and ζ with literature values determined by independent methods to critically test the "parameter-free" nature of the MM model.

A very extensive set of η_0 data for polyisoprene (PI) stars, having $4 \le f \le 33$ and a wide range of n_e, is given by Fetters et al.[28] Data sets covering a substantial range of n_e also exist for polystyrene (PS) stars ($f = 4$ and 6, from Graessley and Roovers[23]) and polybutadiene (PBd) stars ($f = 4$, from Roovers[22]). Finally, Santangelo et al.[29] recently determined η_0 for two six-arm polyisobutylene (PIB) stars synthesized by living cationic polymerization. All of these data sets (for $n_e > 2$) are displayed in Figure 11, and agree remarkably well with the theory over more than six decades in η_0. To place the data points for stars of a given monomer type in Figure 11, values of ρ and b were taken from the compilation of Fetters et al.,[24] adjusted to the temperatures at which the η_0 values are reported (see Table 2). The remaining two material parameters—G_0 (related to M_e by eq (33)) and ζ—were allowed to float to produce the best match of the data set for each monomer type to the MM theory (exact solution). These fitted values of M_e (G_0) and ζ are given for each polymer in Table 2.

To test the validity of our fitted values of G_0 (M_e) and ζ, we may compare them with literature values determined by independent methods. While G_0 is determined directly from experiment, ζ is typically calculated from the viscosity of unentangled linear polymers via[25,30]

$$\zeta = \frac{36\eta_0 m_0}{\rho N_A N b^2} \tag{34}$$

where N is the degree of polymerization and N_A is Avogadro's number. To maintain internal consistency, recent literature values of ζ for PS,[30] PBd,[24] and PI[30] were slightly adjusted according to the values of b in Table 2; for PS and PI, small corrections to the literature values were also made for the molecular weight dependence of the glass transition temperature, as discussed in the Appendix. PIB has been less extensively studied; the literature value of ζ was taken directly from Ferry.[25] Our fitted G_0 values compare very well with those reported by Fetters et al.,[24] within 10% for PBd, PS, and PIB. The discrepancy for PI is larger (20%); however, our fitted value of 0.44 MPa at 333K agrees precisely with that reported by Pearson et al.[31] The fitted values of ζ are also in good agreement with the literature: within a factor of 1.7 for all polymers and within a factor of 1.3 for PBd and PS. Notably, there is no systematic discrepancy between the fitted and literature values of ζ—that is, the need to systematically raise literature values of ζ by a factor of 2 to obtain good agreement with experiment[8,14,17] has been removed by computing the exact solution to the MM model. This suggests that the modest remaining discrepancies result from experimental uncertainty rather than any systematic under- or overprediction of η_0 by the MM theory. The ability to effectively superpose data for well-characterized stars formed from four distinctly different monomers, of varying arm numbers, demonstrates the universality of the MM treatment.

Conclusions

The MM theory[14] provides an excellent description of the dynamics of star molecules. In the original solution, the FPT was approximated by expressions valid in the limit of high n_e, higher than can be accessed experimentally—yet the approximate solution provides a good description of experimental data.[14,17] By developing an exact solution to the FPT and comparing it with the approximate solution presented previously,[14] we have shown that the arm retraction potentials predicted by the approximate and exact solutions have quite different shapes. However, both scale similarly with n_e and yield values of τ_0 which differ by only a factor of 2, so good agreement with experimental quantities in the terminal region can be achieved simply through a corresponding adjustment in the monomeric friction coefficient ζ. Even in the crossover region between short-time (Rouse) and long-time (arm retraction) dynamics, the MM theory (employing an ad hoc crossover formula) gives a good description of the experimental scaling of $G''(\omega_{max})$ with n_e, requiring only a modest modulus shift for quantitative agreement.

The MM theory predicts a slightly stronger dependence of J_e^0 on molecular weight ($J_e^0 \sim n_e^{1.3}$) than does the well-known Pearson-Helfand theory for star relaxation in a fixed network ($J_e^0 \sim n_e^1$); the MM theory provides at least as good a representation of literature data for J_e^0. The MM theory accurately captures the

well-known exponential dependence of η_0 on n_e; compared with the PH theory, the MM theory has a slightly smaller exponential factor ($\phi \approx 0.48$ vs 0.6) and stronger power-law preexponential factor ($\beta = 0.72$ vs $^1/_2$). The MM theory predicts that $\tau_0/J_e^0\eta_0 \approx 3.2$ with a weak n_e dependence, significantly larger than the value of $\approx$1 for monodisperse linear polymers and the value of 2 predicted by the DK and PH theories. Finally, we compared literature η_0 data for star polymers made from four monomers (polyisoprene, polystyrene, polybutadiene, and polyisobutylene) with the theory. Quantitative agreement for all four systems was obtained with values of G_0 (or M_e) in excellent agreement with literature, and with ζ values within the range (factors of 0.7−1.7) of corresponding literature values.

Appendix

The ζ values reported by Chapman[30] correspond to polystyrene and polyisoprene homopolymers with molecular weights of order 10^4 g/mol. Since these polymers do not have glass transition temperatures (T_g) quite equal to the limiting values at high molecular weights (T_g^∞), to obtain the desired ζ values for high-M polymer, a small correction[32] must be made such that the ζ values correspond to equal distances from T_g. The molecular weight dependence of T_g is adequately represented by

$$\Delta T_g = T_g^\infty - T_g = K/M_n \qquad \text{(A1)}$$

where M_n is the number-average molecular weight and K is a material-dependent constant. For polystyrene,[33] $K = 79\,000$ g/mol; for high-1,4 polyisoprene,[34] $K = 17\,600$ g/mol. At the temperatures employed in Table 1 and with the M_n values for the polymers employed by Chapman,[30] these corrections amount to +0.27 in log ζ for polystyrene, and a mere +0.05 in log ζ for polyisoprene. The "literature" values in Table 2 include these corrections.

For the stars whose viscosity data are shown in Figure 11, this correction turns out to be negligible. Roovers and Toporowski[35] report ΔT_g values for several low-molecular-weight polystyrene stars; these are consistent with eq A1 and $K = 79\,000$ g/mol provided the "span" molecular weight ($2M_a$) is used in place of M_n. This idea[35] follows the original Fox−Flory notion[36] that each chain end contributes an extra increment of free volume. By this method, the calculated corrections to log ζ are < 0.02 for the lowest-n_e polyisoprene star in Figure 11, and < 0.03 for the lowest-n_e polystyrene star. These corrections are far smaller than the fit errors in log ζ (see Table 2) and were consequently neglected.

Acknowledgment. This work was supported by the National Science Foundation through the Princeton Center for Complex Materials (DMR-9802468). We thank Professor William W. Graessley for stimulating discussions. D.A.V. gratefully acknowledges support from the National Research Council of Argentina (CONICET) and the Universidad Nacional del Sur.

References and Notes

(1) de Gennes, P. G. *Scaling Concepts in Polymer Physics*; Cornell University Press: Ithaca, NY, 1979.
(2) Doi, M.; Edwards, S. F. *J. Chem. Soc., Faraday Trans. 2* **1978**, *74*, 1802.
(3) Doi, M.; Edwards, S. F. *J. Chem. Soc., Faraday Trans. 2* **1978**, *74*, 1818.
(4) Doi, M.; Edwards, S. F. *The Theory of Polymer Dynamics*; Clarendon Press: Oxford, U.K., 1986.
(5) Doi, M.; Kuzuu, N. *J. Polym. Sci., Polym. Phys. Ed.* **1980**, *18*, 775.
(6) Pearson, D. S.; Helfand, E. *Macromolecules* **1984**, *17*, 888.
(7) Graessley, W. W. *Macromolecules* **1982**, *15*, 1164.
(8) Kapnistos, M.; Semenov, A.; Vlassopoulos, D.; Roovers, J. *J. Chem. Phys.* **1999**, *111*, 1753.
(9) McLeish, T. C. B.; Larson, R. G. *J. Rheol.* **1998**, *42*, 81.
(10) McLeish, T.; Allgaier, J.; Bick, D.; Bishko, G.; Biswas, P.; Blackwell, R.; Blottiere, B.; Clarke, N.; Gibbs, B.; Grovers, D.; Hakiki, A.; Heenan, R.; Johnson, J.; Kant, R.; Read, D.; Young, R. *Macromolecules* **1999**, *32*, 6734.
(11) Curro, J. G.; Pearson, D. S.; Helfand, E. *Macromolecules* **1985**, *18*, 1157.
(12) Vega, D. A.; Villar, M. A.; Alessandrini, J. L.; Valles, E. M. *Macromolecules* **2001**, *34*, 4591.
(13) Ball, R. C.; McLeish, T. C. B. *Macromolecules* **1989**, *22*, 1911.
(14) Milner, S. T.; McLeish, T. C. B. *Macromolecules* **1997**, *30*, 2159.
(15) Watanabe, H. *Prog. Polym. Sci.* **2000**, *24*, 1253.
(16) Milner, S. T.; McLeish, T. C. B.; Young, R. N.; Hakiki, A.; Johnson, J. M. *Macromolecules* **1998**, *31*, 9345.
(17) Milner, S. T.; McLeish, T. C. B. *Macromolecules* **1998**, *31*, 7479.
(18) Colby R.; Rubinstein M. *Macromolecules* **1990**, *23*, 2753.
(19) McLeish, T. C. B.; Milner, S. T. *Adv. Polym. Sci.* **1999**, *43*, 195.
(20) Gradshteyn, I. S.; Ryzhik, I. M. *Table of Integrals, Series and Products*; Jeffrey, A., Ed.; Academic Press: San Diego, CA, 1996.
(21) Helfand, E.; Pearson, D. S. *J. Chem. Phys.* **1983**, *79*, 2054.
(22) Roovers, J. *Polymer* **1985**, *26*, 1091.
(23) Graessley, W. W.; Roovers, J. *Macromolecules* **1979**, *12*, 959.
(24) Fetters, L. J.; Lohse, D. J.; Richter, D.; Witten, T. A.; Zirkel, A. *Macromolecules* **1994**, *27*, 4639 and references therein.
(25) Ferry, J. D. *Viscoelastic Properties of Polymers*, 3rd ed.; Wiley: New York, 1980.
(26) Roovers, J. *Macromolecules* **1991**, *24*, 5895.
(27) Pakula, T.; Vlassopoulos, D.; Fytas, G.; Roovers, J. *Macromolecules* **1998**, *31*, 8931.
(28) Fetters, L. J.; Kiss, A. D.; Pearson, D. S.; Quack, G. F.; Vitus, F. J. *Macromolecules* **1993**, *26*, 647.
(29) Santangelo, P. G.; Roland, C. M.; Puskas, J. E. *Macromolecules* **1999**, *32*, 1972.
(30) Chapman, B. R.; Hamersky, M. W.; Milhaupt, J. M.; Kostelecky, C.; Lodge T. P.; Meerwall, E. D.; Smith, S. D. *Macromolecules* **1998**, *31*, 4562.
(31) Pearson, D. S.; Muller, S. J.; Fetters, L. J.; Hadjichristidis, N. *J. Polym. Sci., Polym. Phys. Ed.* **1983**, *21*, 2287.
(32) Berry, G. C.; Fox, T. G. *Adv. Polym. Sci.* **1968**, *5*, 261.
(33) O'Driscoll, K.; Sanayei, R. A. *Macromolecules* **1991**, *24*, 4479.
(34) Kow, C.; Morton, M.; Fetters, L. J.; Hadjichristidis, N. *Rubber Chem. Technol.* **1982**, *55*, 245.
(35) Roovers, J. E. L.; Toporowski, P. M. *J. Appl. Polym. Sci.* **1974**, *18*, 1685.
(36) Fox, T. G.; Flory, P. J. *J. Appl. Phys.* **1950**, *21*, 581.

MA011501N